Eur Biophys J (2011) 40:209–215
DOI 10.1007/s00249-010-0632-9

BIOPHYSICS LETTER

Quantification of the effect of glycocalyx condition on membrane receptor interactions using an acoustic wave sensor

Michael Saitakis · Electra Gizeli

Received: 23 April 2010 / Revised: 16 July 2010 / Accepted: 28 September 2010 / Published online: 17 October 2010

Abstract The effect of the cell glycocalyx on the binding of a membrane receptor, class I major histocompatibility complex (MHC) human leukocyte antigen (HLA)-A2, to an immobilized anti-HLA antibody was investigated using an acoustic sensor based on a Love wave geometry. The enzyme neuraminidase was used to remove sialic acid residues from the cell glycocalyx. Real-time measurements of the amplitude of the acoustic wave showed that treatment with neuraminidase facilitates HLA/anti-HLA-mediated cell attachment via a 3.6-fold increase of the two-dimensional (2D) binding constant of the interaction. This could be attributed to better approach of binding partners due to favorable condition of the desialylated glycocalyx. The results underline the importance of microtopological factors in membrane receptor binding and reveal the potential of the Love wave sensor and 2D binding parameters for studying cell–substrate binding events.

Keywords Glycocalyx · HLA · SAW sensor · Two-dimensional kinetics · Two-dimensional affinity

Introduction

The binding of cell membrane proteins to their ligands requires the formation of a close contact zone between the apposing surfaces. However, the cell membrane is a complex structure with many different molecules. The specific binding of a receptor–ligand pair between two cell surfaces has to overcome local microtopological constraints from other proteins or glycans. For most cells, a glycocalyx (at least 20 nm deep) exists at the cell surface and forms a negatively charged "cloud." The negative charge mainly originates from the sialic acid residues of the glycoproteins and glycolipids of the cell membrane. This structure can impose limitations on the binding of cell membrane proteins to their ligands, since there has to be local glycocalyx deformation for effective approach and interaction of receptor and ligand to take place (Bell et al. 1984; Shaw and Dustin 1997; Springer 1990; van der Merwe et al. 1994). The extracellular part of the class I major histocompatibility complex molecule HLA-A2 molecules is 7 nm long, a small size compared with other molecules that are present at the lymphocyte membrane. Moreover, it has to interact with the T cell receptor (TCR) on the surface of T cells, a membrane molecule of similar size. In such conditions, the glycocalyx, among other factors such as protein clustering and lateral diffusion (Bodnar et al. 2003; Fooksman et al. 2006; Oh et al. 2001), is expected to play an important role in regulating the interaction of binding partners.

Biosensors can be powerful tools for biophysical study of binding mechanisms of cell membrane molecules, as they can allow noninvasive quantitative monitoring of interactions as well as determination of both kinetics and affinity constants (Cooper 2002, 2006; Cooper and Singleton 2007; Gronewold 2007; Lakey and Raggett 1998). In particular, acoustic biosensors can be extremely advantageous for studying cell-related events such as cell adhesion and motility, since they respond not only to net mass changes but also to differences in the physiological conditions of surface-bound cells (Heitmann et al. 2007;

M. Saitakis · E. Gizeli (✉)
Institute of Molecular Biology and Biotechnology,
FO.R.T.H, 71110 Heraklion, Greece
e-mail: gizeli@imbb.forth.gr

M. Saitakis · E. Gizeli
Department of Biology, University of Crete,
71409 Heraklion, Greece

Wegener et al. 1998, 2000); the latter are monitored as changes in the viscosity of the sensing samples (Janshoff et al. 1996; Li et al. 2005).

One acoustic sensor configuration with particular potential for cell-related studies is the Love wave biosensor. This sensor operates through the use of a polymer waveguide layer that confines the acoustic energy to the sensing surface, resulting in high sensitivity to surface perturbations (Gizeli et al. 2003). In our group, we have developed such a biosensor, which was successfully used to sense mass and viscosity changes via measurements of the phase and amplitude of the acoustic wave, respectively (Melzak et al. 2002; Mitsakakis et al. 2009; Tsortos et al. 2008a, b). Specifically, amplitude measurements were used to monitor the process of cell attachment and spreading (Saitakis et al. 2008, 2010). It was shown that amplitude change is proportional to the number of bonds formed between cell membrane HLA and immobilized anti-HLA (Saitakis et al. 2008, 2010); the latter finding enabled calculation of two-dimensional (2D) kinetics and affinity constants of the interaction from real-time data (Saitakis et al. 2008), providing quantitative data and insight into cellular binding events (Alon et al. 1997; Bromley et al. 2001; Dustin et al. 1996, 1997).

In this work, the Love wave biosensor is applied to study the effect of glycocalyx condition on cell membrane molecule interactions. As a model system, the class I MHC molecule human leukocyte antigen (HLA)-A2 on the surface of live cells and an anti-HLA-A2 antibody were used. The attachment of HLA-expressing cells to the sensor surface, modified with the anti-HLA antibody, was monitored in real time using the acoustic biosensor. The effect of the glycocalyx was probed after treatment of cells with the enzyme neuraminidase, which cleaves sialic acid residues from cell surface glycans, while the 2D kinetic parameters and the binding affinity were calculated from real-time binding curves.

Materials and methods

Cell cultures and treatments

The Epstein–Barr virus (EBV)-transformed human B-lymphoblastoid cell line LG2 (HLA-A*0201$^{+/+}$) was used in this work. Roswell Park Memorial Institute (RPMI) 1640 (GIBCO Inc.) supplemented with 1 mg l^{-1} gentamicin and 10% of fetal bovine serum was used as culture medium. Culture flasks were kept in humidified 5% CO_2 atmosphere at 37°C. Medium was exchanged every 2–3 days. Viability was checked prior to experiments by the trypan blue exclusion technique, and cell number was counted on a Neubauer slide. Dead cells were never over 5% of the total. Cells were washed with phosphate-buffered saline (PBS; Sigma), centrifuged at 250 × g, and resuspended in PBS prior to addition to the sensor surface. Cell density was 3–8 × 10^5 cells ml^{-1} in normal cultures and 2–3 × 10^6 cells ml^{-1} in high-density cultures.

Neuraminidase (New England Biolabs) treatment of cells comprised 40-min incubation of LG2 cells at 37°C with 100 U ml^{-1} enzyme. Cells were then washed twice with PBS (Sigma). Negative controls received the same treatment in the absence of the enzyme.

Love wave sensor setup, surface preparation, and real-time acoustic experiments

The acoustic waveguide device, operating at 110 MHz, has been extensively described elsewhere (Gizeli et al. 2003; Saha et al. 2003; Saitakis et al. 2008; Tsortos et al. 2008b). Briefly, the apparatus comprises a quartz crystal device which utilizes a set of interdigitated transducers (IDTs) to generate and detect a shear-horizontal surface acoustic wave (SH-SAW). The phase and amplitude of the acoustic wave, which are related to the acoustic velocity and energy, respectively, are measured as a function of time. All sensing occurs only within the liquid layer in contact with the device, within a distance of 50 nm for an aqueous solution. A gold layer on top of the sensor chip serves as a surface that allows immobilization of the biorecognition layer. Gold device surfaces were plasma-etched in oxygen plasma (Plasma Etcher, Harrick).

Gold-coated device surfaces were incubated with a protein G (Calbiochem) solution (1 mg ml^{-1}) which was left to adsorb for 1 h at room temperature. Protein G, which adsorbs irreversibly onto gold, was used to specifically bind antibodies via their Fc fragment, resulting in oriented immobilization (Saha et al. 2003). Following protein adsorption, the device was inserted into the device holder, washed, and left to equilibrate with PBS (Sigma) at flow rate of 50 µl min^{-1}. The anti-HLA-A2 monoclonal antibody BB7.2 (Becton–Dickinson), which recognizes the α-chain of HLA when the latter exists in heterotrimer form of α-chain, β_2-microglobulin, and a bound peptide (Hogan and Brown 1992; Parham and Brodsky 1981), was then added and immobilized onto the sensor surface. It was shown that anti-HLA adsorbed onto the sensor surface under these conditions forms a dense layer, with surface density of 5.9 ± 1.9 × 10^3 molecules µm^{-2}, which promotes cell attachment and spreading (Saitakis et al. 2008). All experiments were performed at 25°C. Cell suspensions were added under flow (10 µl min^{-1}) over the anti-HLA-modified sensor surface; the real-time binding curves for amplitude change were obtained and processed. Following the end of an acoustic experiment, the biosensor surface was observed under the microscope. Since the sensor chip

is not opaque, no fluorescent staining was needed for the observation of cells. The surface was observed under a Nikon Eclipse E800 microscope, and pictures were taken with an attached ProgRes CF camera (Jenoptik).

Two-dimensional kinetic analysis of real-time acoustic data

Real-time binding curves from experiments with different cell suspensions and glycocalyx conditions were collected and processed as described before (Saitakis et al. 2008). Briefly, the analysis is based on the following equation:

$$\Delta(\mathrm{d}A/\mathrm{d}t)/\Delta A = k_{\mathrm{a}}C^{2\mathrm{D}} + k_{\mathrm{d}},$$

where $\Delta(\mathrm{d}A/\mathrm{d}t)$ and ΔA are the change in the rate and overall amplitude, respectively, derived from real-time graphs, $C^{2\mathrm{D}}$ is the effective surface density of the cell membrane molecule, and k_{a} and k_{d} are the two-dimensional association and dissociation rate constants, respectively. The effective surface density $C^{2\mathrm{D}}$ was calculated from the HLA surface density of each cell type (374 ± 80 molecules $\mu\mathrm{m}^{-2}$ for untreated and neuraminidase-treated cells, and 694 ± 21 molecules $\mu\mathrm{m}^{-2}$ for cells from high-density cultures) and the sensor surface coverage by cells (measured from microscopy photos). The real-time data for cell attachment (from sample time $t = 500$ s up to equilibrium condition) were fitted to a single exponential curve. This part of the graph mainly reflects the formation of new HLA/anti-HLA bonds (Saitakis et al. 2008). From the fitted curves, the rate in amplitude change was calculated as a function of time and plotted versus ΔA. Plotting the slopes of the above curves, i.e., $\Delta(\mathrm{d}A/\mathrm{d}t)/\Delta A$, versus the effective HLA surface density $C^{2\mathrm{D}}$ enables measurement of the 2D association and dissociation rate constants: k_{a} from the slope and k_{d} from the intercept with the ordinate. The 2D binding affinity K_{A} was then calculated as $K_{\mathrm{A}} = k_{\mathrm{a}}/k_{\mathrm{d}}$. The data were analyzed using Microcal Origin 6.1 software.

Flow cytometry

LG2 cells were incubated with the anti-HLA-A2 monoclonal antibody BB7.2 (Becton–Dickinson) and fluorescein isothiocyanate-conjugated anti-mouse IgG (as a secondary fluorescence-activated cell sorter antibody) (Dako), both at saturating conditions. Samples were analyzed in a fluorescence-activated cell sorter (FACS) scanner (FACScanner; Becton Dickinson). Light-scattering and fluorescein isothiocyanate fluorescence data were collected on four-decade logarithmic scales, and the mean fluorescence intensity for each sample was deduced. Moreover, using an indirect quantitative immunofluorescence assay (QIFIKIT, Dako), the number of HLA heterotrimers on the cell surface was calculated. The values were: 3.7–5.7 × 10^5 HLA molecules per untreated LG2 cell and 9.7–10.0 × 10^5 per LG2 cell from a high-density culture.

Results

Real-time acoustic experiments of cell attachment for untreated and neuraminidase-treated cells

LG2 cells are tumor cells derived from the B-lymphoblastoid line, and their cell membrane is covered by an extensively sialylated glycocalyx (Fuster and Esko 2005; Hollingsworth and Swanson 2004; Shaw and Dustin 1997). To probe the effect of the glycocalyx, a neuraminidase incubation step was used as a treatment to assay the effect of a desialylated glycocalyx on cell attachment to the sensor surface. First, to check whether neuraminidase treatment affects HLA-A2 binding to the anti-HLA antibody, flow cytometry experiments were performed with LG2 cells incubated with anti-HLA. The results showed that soluble anti-HLA binding is not affected by neuraminidase treatment. Moreover, the number of HLA molecules per each cell was the same (3.7–5.7 × 10^5 per cell). The two types of LG2 cells, i.e., untreated and neuraminidase treated, were then applied in real-time acoustic experiments over the protein G/anti-HLA-modified sensor surface (Fig. 1) at various cell numbers. The attachment and spreading of LG2 cells on the sensor surface resulted in real-time sigmoid-like binding curves (Fig. 2). Binding related to the first part of the graph (∼first 500 s) is associated to cell diffusion and initial cell

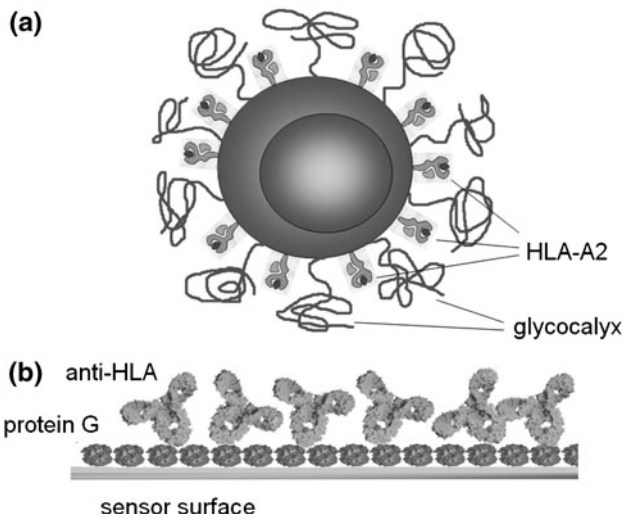

Fig. 1 Schematic representation of **a** LG2 cells with HLA molecules surrounded by various glycans (glycocalyx) on the cell membrane, and **b** the protein G/anti-HLA-modified sensor surface (not to scale)

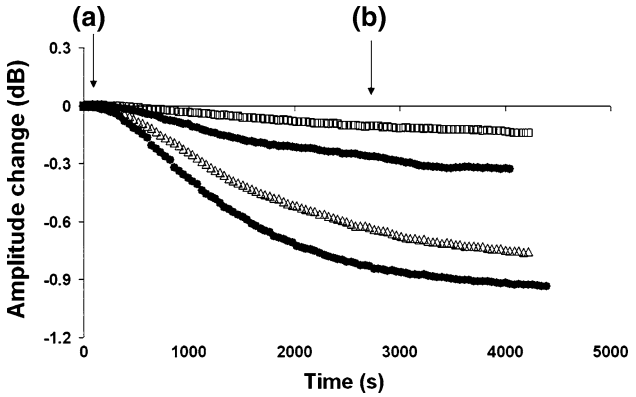

Fig. 2 Real-time acoustic experiments for neuraminidase-treated cells. Cell numbers: 1×10^5 cells ml^{-1} (*open squares*), 2×10^5 cells ml^{-1} (*filled rhombs*), 3×10^5 cells ml^{-1} (*open triangles*), and 5×10^5 cells ml^{-1} (*filled circles*). *Arrows* indicate injection of cell sample (*a*) and exchange with buffer (*b*)

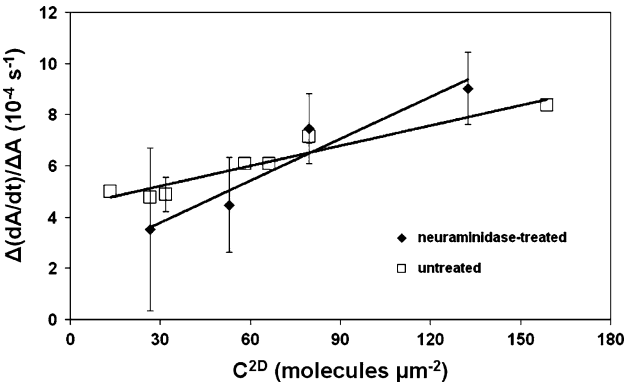

Fig. 3 Plot of $\Delta(dA/dt)/\Delta A$, where (dA/dt) and ΔA are the rate and corresponding amplitude change derived from real-time curves and $\Delta(dA/dt)/\Delta A$ is the slope of (dA/dt) against ΔA, versus the effective HLA surface density C^{2D} for the conditions of untreated and neuraminidase-treated LG2 cells. k_a^{2D} is calculated from the slope and k_d^{2D} from the intercept with the ordinate. These values are presented in Table 1

tethering, while binding related to the second part of the curve is attributed to the formation of new HLA/antibody bonds as a result of further binding between the cell and the surface (Saitakis et al. 2008). The overall signal change has been shown to correlate directly to the number of cell-surface attachment points, which in turn is a measure of two parameters: the number of bound cells and the surface density of cell membrane HLA.

Two-dimensional kinetic analysis of cell membrane HLA/immobilized anti-HLA interaction

To quantify the binding process and determine how the neuraminidase treatment affects the cell attachment, the real-time acoustic data were further analyzed to deduce the 2D kinetics and affinity for the interaction for both untreated and neuraminidase-treated LG2 cells. Cell numbers ranging from 0.6 to 6×10^5 cells ml^{-1} were used for untreated cells and from 1 to 5×10^5 cells ml^{-1} for neuraminidase-treated cells. These cell numbers resulted in different effective HLA surface densities (C^{2D}) on the sensor surface. The kinetic and affinity constants were deduced by plotting the differential of response rate against the effective HLA surface densities (C^{2D}) for each cell type (Fig. 3). The neuraminidase treatment resulted in a higher association rate constant (k_a) and binding affinity (K_A) and a lower dissociation rate constant (k_d) compared with untreated as well as high-density-cultured cells (Table 1). For comparison, the 2D binding parameters were determined for LG2 cells cultured at high densities, a treatment that doubles the number of HLA heterotrimers at the cell surface, using cell numbers ranging form 0.75 to 6×10^5 cells ml^{-1}.

Discussion

The Love wave acoustic biosensor was used in this work to determine the effect of a cell-membrane microtopological factor, the glycocalyx, on a protein–protein interaction mediating specific attachment of LG2 cells onto the sensor surface. Treatment of LG2 cells with the enzyme neuraminidase resulted in sialic acid residue loss from cell surface glycans, which in turn renders the glycocalyx less dense and less negatively charged. From real-time binding curves, this was observed as a sharper binding profile for neuraminidase-treated LG2 cells (data not shown). Moreover, since flow cytometry experiments did not show a difference between untreated and neuraminidase-treated cells for the binding of soluble anti-HLA to the cell surface HLA molecules, it was concluded that the enzyme treatment did not directly affect the protein–protein binding but only affected the interaction at the cell–substrate interface.

Following the above qualitative approach, the effect of the desialylated glycocalyx on specific cell attachment was quantified. This was performed by calculating the two-dimensional association and dissociation rate constants as well as the two-dimensional binding affinity for the HLA/anti-HLA interaction for three states of LG2 cells: untreated, neuraminidase treated, and cultured at high density. The two-dimensional binding parameters are considered biologically more relevant than the traditional three-dimensional binding parameters calculated for soluble molecules. Moreover, they can be used to compare the microtopological and molecular context of cell membrane molecules directly (Bromley et al. 2001; Dustin et al. 2001; Shaw and Dustin 1997).

Table 1 Two-dimensional association rate, dissociation rate, and binding affinity constants for LG2 cells in three different conditions

	k_a (μm^2 s^{-1} per molecule)	k_d (s^{-1})	K_A (μm^2 per molecule)
Untreated	2.77×10^{-6}	4.36×10^{-4}	0.0064
Neuraminidase treated	5.33×10^{-6}	2.30×10^{-4}	0.0232
High-density cultures	4.04×10^{-6}	2.74×10^{-4}	0.0147

All values have an average 10% error. Untreated ($n = 7$), neuraminidase treated ($n = 4$), high-density cultures ($n = 5$)

According to Table 1, the 2D binding affinity for neuraminidase-treated cells is 3.6-fold higher than for untreated cells[1] and 1.5-fold higher than cells from high-density cultures. The above suggest the following: cutting down the glycocalyx with neuraminidase facilitated the protein–protein interaction at the cell–substrate interface to a higher degree than even doubling the number of binding partners. This was also observed from the faster 2D association rate constant with neuraminidase treatment. The latter could be attributed to easier deformation of the less dense glycocalyx during the formation of HLA/anti-HLA bonds. Furthermore, the lower repulsion due to charge and the lower glycan density should exert less pressure on the already formed HLA/anti-HLA bonds, which was also observed as a lowered 2D dissociation rate constant for neuraminidase-treated LG2 cells.

At the sensor surface, during contact area formation, HLA molecules present in the membrane apposed to the sensor surface readily interact with the immobilized anti-HLA molecules. The fast lateral diffusion of HLA molecules on the cell membrane (Bierer et al. 1987) is much faster than the binding rate of the probed interaction, allowing for continuous recruitment of free HLA molecules to the contact area; this process leads to the safe assumption that the HLA surface density for free molecules is constant. In addition, due to the high surface density of anti-HLA molecules ($5.9 \pm 1.9 \times 10^3$ molecules μm^{-2}), there is no restriction on the number of bonds that can be formed between the cell and the sensor surface (maximum HLA surface density at the established contact area is 2.9×10^3 molecules μm^{-2}). Finally, even though dissociation was not observed for whole cells, it can occur for single HLA/anti-HLA bonds; in the current setup, rebinding of the dissociated HLA can readily occur, given the high surface antibody density, and this may bias the k_d towards lower values. The contact area for the three types of cells was observed from microscopy photos to be the same. This was expected since contact area formation is driven by the submembrane actin network of the cells.

In another work, the effect of surface charge on cell attachment was observed acoustically with heparinase treatments of endothelial cells (Ergezen et al. 2007; Hong et al. 2006). Heparinase-treated endothelial cells were applied on a poly-D-lysine-coated acoustic wave device [a thickness shear mode (TSM) resonator], and the adhesion was monitored in real time. The enzyme treatment resulted in lower cell attachment (Ergezen et al. 2007; Hong et al. 2006), since the adhesion on poly-D-lysine is nonspecific and is mediated via electrostatic bonds between the positively charged immobilized poly-D-lysine and the negatively charged cell surface heparan sulfate proteoglycans. In our study, we went one step further to quantify the effect of glycocalyx, and thus the effect of negative charge, using the 2D binding parameters.

The main characteristic of the Love wave sensor technique is that it offers direct measurement of the number of bonds formed between cell and substrate, so that the calculated 2D kinetic rates from the signal change represent HLA/anti-HLA binding. In this context, the Love wave sensor technique presents an important advantage compared with current mechanical and fluorescence methods that are employed for two-dimensional parameter determination. However, with our system, it was not possible to discriminate the effect of lateral diffusion of HLA molecules and/or contact area formation on the HLA/anti-HLA binding. This was in contrast to another work (Tolentino et al. 2008; Wu et al. 2008), where the effect of the biological process of cell spreading was isolated by looking at already established contact areas. Thus, it can be concluded that, for 2D parameter calculation, these techniques can be used complementarily to isolate and elucidate different mechanisms of the biology of cell adhesion.

Overall, the dependence of cell adhesion efficiency on glycocalyx condition was displayed for a cell membrane receptor binding to an immobilized ligand. HLA/anti-HLA binding on the cell substrate interface was more efficient after neuraminidase treatment due to less dense glycocalyx and less surface charge. The results also demonstrate the potential of the Love wave sensor for the study of cellular

[1] The 2D kinetics and affinity of the HLA/anti-HLA interaction for untreated LG2 cells had previously been calculated as $k_a = 1.15 \times 10^{-5}$ μm^2 s^{-1} per molecule, $k_d = 2.07 \times 10^{-5}$ s^{-1}, and $K_A = 0.556$ μm^2 per molecule (Saitakis et al. 2008). In that work, the kinetic analysis was performed for real-time acoustic data up to the point of buffer exchange. In the current study, we included data up to the point of signal equilibrium, since there was still HLA/anti-HLA binding taking place on the sensor surface. We believe that this modification is justified, since it includes the whole real-time data for the association reaction.

events in, e.g., the immune system, which abounds with intercellular interactions that determine the fate of individual cells and immune responses (Huppa and Davis 2003).

Acknowledgments The authors would like to acknowledge the financial support of ELKE, University of Crete (research grant K. A. 2732) and the General Secretariat of Research and Technology (PENED 03ED623).

References

Alon R, Chen S, Puri KD, Finger EB, Springer TA (1997) The kinetics of L-selectin tethers and the mechanics of selectin-mediated rolling. J Cell Biol 138:1169–1180

Bell GI, Dembo M, Bongrand P (1984) Cell adhesion. Competition between nonspecific repulsion and specific bonding. Biophys J 45:1051–1064

Bierer BE, Herrmann SH, Brown CS, Burakoff SJ, Golan DE (1987) Lateral mobility of class I histocompatibility antigens in B lymphoblastoid cell membranes: modulation by cross-linking and effect of cell density. J Cell Biol 105:1147–1152

Bodnar A, Bacso Z, Jenei A, Jovin TM, Edidin M, Damjanovich S, Matko J (2003) Class I HLA oligomerization at the surface of B cells is controlled by exogenous beta(2)-microglobulin: implications in activation of cytotoxic T lymphocytes. Int Immunol 15:331–339

Bromley SK, Iaboni A, Davis SJ, Whitty A, Green JM, Shaw AS, Weiss A, Dustin ML (2001) The immunological synapse and CD28-CD80 interactions. Nat Immunol 2:1159–1166

Cooper MA (2002) Optical biosensors in drug discovery. Nat Rev Drug Discov 1:515–528

Cooper MA (2006) Non-optical screening platforms: the next wave in labal-free screening? Drug Discov Today 11:1068–1074

Cooper MA, Singleton VT (2007) A survey of the 2001 to 2005 quartz crystal microbalance biosensor literature: applications of acoustic physics to the analysis of biomolecular interactions. J Mol Recognit 20:154–184

Dustin ML, Ferguson LM, Chan PY, Springer TA, Golan DE (1996) Visualization of CD2 interaction with LFA-3 and determination of the two-dimensional dissociation constant for adhesion receptors in a contact area. J Cell Biol 132:465–474

Dustin ML, Golan DE, Zhu DM, Miller JM, Meier W, Davies EA, van der Merwe PA (1997) Low affinity interaction of human or rat T cell adhesion molecule CD2 with its ligand aligns adhering membranes to achieve high physiological affinity. J Biol Chem 272:30889–30898

Dustin ML, Bromley SK, Davis MM, Zhu C (2001) Identification of self through two-dimensional chemistry and synapses. Annu Rev Cell Dev Biol 17:133–157

Ergezen E, Hong S, Barbee KA, Lec R (2007) Real time monitoring of the effects of heparan sulfate proteoglycan (HSPG) and surface charge on the cell adhesion process using thickness shear mode (TSM) sensor. Biosens Bioelectron 22:2256–2260

Fooksman DR, Gronvall GK, Tang Q, Edidin M (2006) Clustering class I MHC modulates sensitivity of T cell recognition. J Immunol 176:6673–6680

Fuster MM, Esko JD (2005) The sweet and sour of cancer: glycans as novel therapeutic targets. Nat Rev Cancer 5:526–542

Gizeli E, Bender F, Rasmusson A, Saha K, Josse F, Cernosek R (2003) Sensitivity of the acoustic waveguide biosensor to protein binding as a function of the waveguide properties. Biosens Bioelectron 18:1399–1406

Gronewold TM (2007) Surface acoustic wave sensors in the bioanalytical field: recent trends and challenges. Anal Chim Acta 603:119–128

Heitmann V, Reiss B, Wegener J (2007) The quartz crystal microbalance in cell biology: basics and applications. In: Steinem C, Janshoff A (eds) Piezoelectric sensors. Springer, Berlin, pp 303–338

Hogan KT, Brown SL (1992) Localization and characterization of serologic epitopes on HLA-A2. Hum Immunol 33:185–192

Hollingsworth MA, Swanson BJ (2004) Mucins in cancer: protection and control of the cell surface. Nat Rev Cancer 4:45–60

Hong S, Ergezen E, Lec R, Barbee KA (2006) Real-time analysis of cell-surface adhesive interactions using thickness shear mode resonator. Biomaterials 27:5813–5820

Huppa JB, Davis MM (2003) T-cell-antigen recognition and the immunological synapse. Nat Rev Immunol 3:973–983

Janshoff A, Wegener J, Sieber M, Galla HJ (1996) Double-mode impedance analysis of epithelial cell monolayers cultured on shear wave resonators. Eur Biophys J 25:93–103

Lakey JH, Raggett EM (1998) Measuring protein–protein interactions. Curr Opin Struct Biol 8:119–123

Li J, Thielemann C, Reuning U, Johannsmann D (2005) Monitoring of integrin-mediated adhesion of human ovarian cancer cells to model protein surfaces by quartz crystal resonators: evaluation in the impedance analysis mode. Biosens Bioelectron 20: 1333–1340

Melzak K, Martin F, Newton MI, McHale G, Gizeli E (2002) Acoustic determination of polymer molecular weights and rotation times. J Polymer Sci B Polym Phys 40:1490–1495

Mitsakakis K, Tsortos A, Kondoh J, Gizeli E (2009) Parametric study of SH-SAW device response to various types of surface perturbations. Sens Actuators B Chem 138:408–416

Oh S, Belz GT, Eichelberger MC (2001) Viral neuraminidase treatment of dendritic cells enhances antigen-specific CD8(+) T cell proliferation, but does not account for the CD4(+) T cell independence of the CD8(+) T cell response during influenza virus infection. Virology 286:403–411

Parham P, Brodsky FM (1981) Partial purification and some properties of BB7.2. A cytotoxic monoclonal antibody with specificity for HLA-A2 and a variant of HLA-A28. Hum Immunol 3:277–299

Saha K, Bender F, Gizeli E (2003) Comparative study of IgG binding to proteins G and A: nonequilibrium kinetic and binding constant determination with the acoustic waveguide device. Anal Chem 75:835–842

Saitakis M, Dellaporta A, Gizeli E (2008) Measurement of two-dimensional binding constants between cell-bound major histocompatibility complex and immobilized antibodies with an acoustic biosensor. Biophys J 95:4963–4971

Saitakis M, Tsortos A, Gizeli E (2010) Probing the interaction of a membrane receptor with a surface-attached ligand using whole cells on acoustic biosensors. Biosens Bioelectron 25:1688–1693

Shaw AS, Dustin ML (1997) Making the T cell receptor go the distance: a topological view of T cell activation. Immunity 6:361–369

Springer TA (1990) Adhesion receptors of the immune system. Nature 346:425–434

Tolentino TP, Wu J, Zarnitsyna VI, Fang Y, Dustin ML, Zhu C (2008) Measuring diffusion and binding kinetics by contact area FRAP. Biophys J 95:920–930

Tsortos A, Papadakis G, Gizeli E (2008a) Shear acoustic wave biosensor for detecting DNA intrinsic viscosity and conformation: a study with QCM-D. Biosens Bioelectron 24:836–841

Tsortos A, Papadakis G, Mitsakakis K, Melzak KA, Gizeli E (2008b) Quantitative determination of size and shape of surface-bound DNA using an acoustic wave sensor. Biophys J 94:2706–2715

van der Merwe PA, Barclay AN, Mason DW, Davies EA, Morgan BP, Tone M, Krishnam AK, Ianelli C, Davis SJ (1994) Human cell-adhesion molecule CD2 binds CD58 (LFA-3) with a very low affinity and an extremely fast dissociation rate but does not bind CD48 or CD59. Biochemistry 33:10149–10160

Wegener J, Janshoff A, Galla HJ (1998) Cell adhesion monitoring using a quartz crystal microbalance: comparative analysis of different mammalian cell lines. Eur Biophys J 28:26–37

Wegener J, Seebach J, Janshoff A, Galla HJ (2000) Analysis of the composite response of shear wave resonators to the attachment of mammalian cells. Biophys J 78:2821–2833

Wu J, Fang Y, Zarnitsyna VI, Tolentino TP, Dustin ML, Zhu C (2008) A coupled diffusion-kinetics model for analysis of contact-area FRAP experiment. Biophys J 95:910–919